DOI: https://doi.org/10.24425/amm.2025.153474

A. ZIĘBA[1*], Ł. ROGAL[1], D. DURACZYŃSKA[2], A. GÓRAL[1],
K. STAN-GŁOWIŃSKA[1], L. LITYŃSKA DOBRZYŃSKA[1]

MICROSTRUCTURE AND CATALYTIC PROPERTIES OF Al-Ni-Fe ALLOYS IN THE FORM OF MELT-SPUN RIBBONS

In this study, the microstructure and catalytic potential of two Al-Ni-Fe alloys synthesised through a melt-spinning process with compositions selected to favour quasicrystalline phase formation were investigated. Microstructural and chemical analyses performed using X-ray diffraction, scanning and transmission electron microscopy methods revealed complex morphology and multiphase composition for both alloys. The presence of a decagonal quasicrystalline phase in both materials and additional crystalline phases occurring along the grain boundaries was confirmed. The catalytic potential of alloys was explored in the phenylacetylene hydrogenation reaction. The $Al_{70}Ni_{15}Fe_{15}$ catalyst demonstrated catalytic activity with over 90% phenylacetylene conversion and selectivity to styrene exceeding 50% for styrene production under mild reaction conditions, and $Al_{71.5}Ni_{23.5}Fe_5$ alloy provided the substrate conversion of 46% and selectivity over 50%. The presented results provide insight into the experimental verification of the properties of the new sustainable catalyst solutions.

Keywords: Melt spinning; intermetallic phases; quasicrystal; catalysis; microstructure characterisation

1. Introduction

Quasicrystals exhibit unique structures with a lack of translational symmetry that impart specific material properties, making them promising development options for construction and functional materials [1]. The surfaces of quasicrystals possess distinctive electronic structures, providing high corrosion resistance [2], which can also be beneficial in catalysis [3]. Aluminium-based quasicrystalline phases and their approximants have been proposed as more available and sustainable alternatives to noble-metal catalysts and precursors for catalysts [4,5]. Notably, Al-Fe and Al-Co systems have been identified as promising catalysts for reactions of semihydrogenation of unsaturated hydrocarbons in a liquid and gas environment [6,7]. Quasicrystals were also successfully used as precursors for leached porous structures applied as catalysts for methanol steam reforming [8].

Theoretical and experimental research suggests a correlation between catalytic activity and surface clusters $TMAl_5$ (TM – transition metal) that occur in quasicrystals and approximants [9]. Significant catalytic properties have been observed in Al-Pd-Ru [10], Al-Cu-Fe [11], and Al-Ni-Co [12] alloys, which have been used as catalysts mainly for hydrogenation reactions and methanol steam reforming. These findings encourage further exploration of catalytically active quasicrystalline materials structurally and compositionally related to quasicrystals and approximants with high catalytic performance. The promising candidates are Al-Fe quasicrystals, which are structurally related to the monoclinic $Al_{13}Fe_4$ approximant [13]. This phase provided comparable substrate conversion and selectivity to ethylene in the reaction of acetylene hydrogenation to industrial benchmark catalyst and higher stability than palladium catalyst, by stable level of conversion for 20 h [14]. In the reaction of butadiene hydrogenation, the $Al_{13}Fe_4$ (010) surface provided the highest butene formation among all tested $Al_{13}TM_4$ phases at room temperature conditions [6]. These promising results encourage the exploration of the potential of structurally related phases, however, binary Al-Fe quasicrystals are thermodynamically unstable, which may lead to degradation of material in the reaction conditions. To achieve a stable phase, the addition of a third element, such as nickel, is necessary [15].

Decagonal quasicrystal in the Al-Ni-Fe system have been observed across a range of compositions $Al_{70\text{-}75}Fe_{4.7\text{-}22}Ni_{3\text{-}23,7}$ (at.%) in alloys produced under both equilibrium and non-equilibrium conditions using various manufacturing methods [2,16].

[1] INSTITUTE OF METALLURGY AND MATERIALS SCIENCE, POLISH ACADEMY OF SCIENCES, 25 REYMONTA STR., 30-059 KRAKOW, POLAND
[2] JERZY HABER INSTITUTE OF CATALYSIS AND SURFACE CHEMISTRY, POLISH ACADEMY OF SCIENCES, KRAKOW, POLAND

* Correspondence author: a.zieba@imim.pl

The melt spinning process is particularly attractive due to the low-temperature instability of this phase [17]. Melt-spun ribbons of quasicrystals are brittle, facilitating their pulverization into fine powders with particle sizes in the micrometre range which provide simple application as a catalyst.

This study aims to produce alloys containing Al-Ni-Fe quasicrystals by melt spinning and evaluate their catalytic properties in the phenylacetylene hydrogenation reaction, thereby expanding the data on the catalytic properties of aluminium-based complex phases. The alloy compositions chosen for this study are based on two specific materials. The first is the $Al_{71}Ni_{24}Fe_5$ decagonal quasicrystal, which formed under nonequilibrium conditions with a cooling rate of 10^3°C/s [2]. The second is the $Al_{72.5}Ni_{13}Fe_{14.5}$ alloy, which was obtained under equilibrium conditions and contains both decagonal quasicrystals and the Al_5FeNi intermetallic phase [16]. The manufacturing process and catalytic tests aim to consist of low energy effort and uncomplicated steps, to provide sustainable and environment friendly potential catalysts.

2. Materials and methods

The chemical composition of alloys was chosen based on the literature reports indicating the occurrence of decagonal quasicrystalline phases under equilibrium and rapid solidification conditions [16,18,19]. The examined alloys with the following compositions: $Al_{70}Ni_{15}Fe_{15}$ and $Al_{71.5}Ni_{23.5}Fe_5$ (in at.%) were designated ANF-1 and ANF-2, respectively. The materials were manufactured by the melt spinning method, using previously prepared ingots cast in the induction furnace from the metals with a purity of 99.9%. The melt spinning process was conducted with the linear speed of the drum 20 m/s and a helium pressure of 1.8 bar. As a result of the process, ribbons in the form of fragmented brittle flakes with a width of 60-100 µm were obtained. Melt-spun ribbons were characterized in terms of microstructure, phase and chemical composition using X-ray diffraction (XRD), scanning electron microscopy (SEM) and transmission electron microscopy (TEM) methods. Phase composition of materials was verified for pulverised ribbons by the Bruker D8 Discover X-ray diffractometer (XRD) with CoKα radiation (1.7903 Å). Microstructure observations were carried out for cross-sections of ribbons in the direction of casting in backscattered electrons mode with FEI E-SEM XL-30 equipped with an energy-dispersive X-ray spectrometer (EDS) with an accelerating voltage of 20 kV. Detailed microstructure study with phase and chemical composition analysis was carried out using FEI Tecnai G2 with an accelerating voltage of 200 kV, which featured a high-angle annular dark-field scanning transmission electron microscopy detector (HAADF-STEM). TEM foils were prepared from the fragments of ribbons using a Tenupol-5 double jet electropolisher with an electrolyte containing nitric acid and methanol in proportion 1:3 at a temperature of –30°C and a voltage of 12 V.

For catalytic performance tests, melt-spun ribbons were pulverized using a vibration ball mill Fritsch Pulversiette0 and sieved by Fritsch Analysette3 vibratory sieve shaker to separate the particle fraction below 32 µm. Tests were carried out in the reaction of phenylacetylene hydrogenation which was chosen as a model reaction of hydrogenation of unsaturated hydrocarbons in a liquid environment. Before the reaction, the powders were immersed in a 2 M $NaBH_4$ aqueous solution providing reduction conditions and were kept there until the hydrogen bubbles ceased to appear. Subsequently, the powders were transferred to the reactor. Tests were performed in an agitated batch glass reactor under mild conditions: temperature of reaction mixture 50°C and hydrogen pressure 5 bar. The reaction mixture contained propan-2-ol as a solvent, 300 mol of phenylacetylene and 50 mg of catalyst. During reactions, the samples of the reaction mixture were collected every 10 minutes, and their composition was evaluated using a Clarius 500, Perkin Elmer gas chromatograph with helium as a carrier gas.

3. Results and discussion

3.1. Materials characterisation

The microstructure of melt-spun ribbons evaluated on the cross-section of the ribbons by scanning electron microscopy method was shown in Fig. 1. For both examined compositions, the ribbons have thickness in the range of 60-100 µm and complex multiphase microstructure. The cross-section of ANF-1 alloy contains equiaxed grains near the wheel side of the ribbon and dendrites and eutectics in the central part and near the free side of the ribbon (Fig. 1a, b). Dendrites with a brighter contrast compared to the matrix are enriched in transition metals. It was found that although the ANF-2 alloy differs from ANF-1 only in the mutual content of nickel and iron, the morphology of the ribbons is significantly modified. The ANF-2 ribbon cross-section contains mainly columnar grains with a second phase enriched in aluminium along column boundaries and, as in the case of the ANF-1 alloy, dendrites occurring in the area near the free surface of the ribbon (Fig. 1c, d). The differences in the microstructural features observed along the thickness of the ribbon indicate the change in cooling rate, which may result from the thickness of the ribbons and is an effect of manufacturing conditions [18]. The EDS analysis verified that ANF-1 has an average chemical composition of Al-67 at.%, Ni-17 at.%, and Fe-16 at.%, while ANF-2 has Al-70 at.%, Ni-24.5 at.%, and Fe-5.5 at.%, which corresponded to the assumed initial ranges.

Phase composition of materials was examined for pulverised ribbons by X-ray diffraction (Fig. 2). The diffractogram of ANF-1 alloy enables the identification of the following phases: decagonal quasicrystalline phase (DQC), monoclinic $Al_{13}Fe_4$ [19], AlNi and Al_5FeNi [16] (Fig. 2a). Modification of the chemical composition and increasing the share of nickel at the expense of iron, introduced in the case of the ANF-2 alloy, led to a significant change in the phase composition. The ANF-2 alloy diffractogram reflection positions were assigned to DQC, Al_9Ni_2 and Al solid solution (Fig. 2b). It can be seen

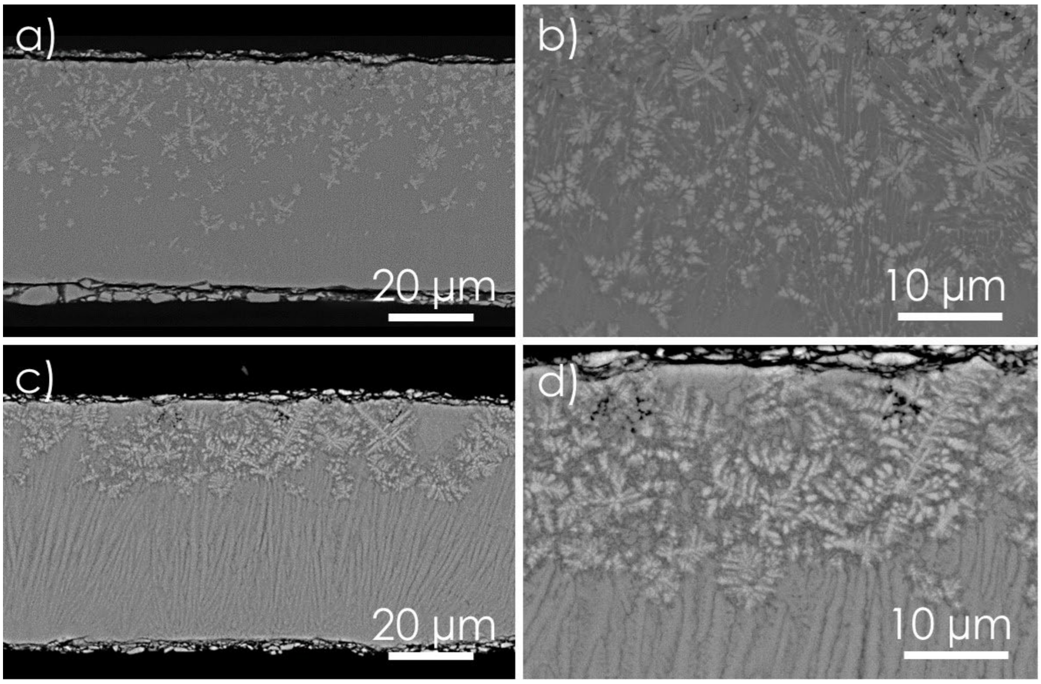

Fig. 1. Microstructure of the cross-section of $Al_{70}Ni_{15}Fe_{15}$ (ANF-1) melt-spun ribbon (a, b) and $Al_{71.5}Ni_{23.5}Fe_5$ (ANF-2) melt-spun ribbon (c, d) acquired using SEM/BSE

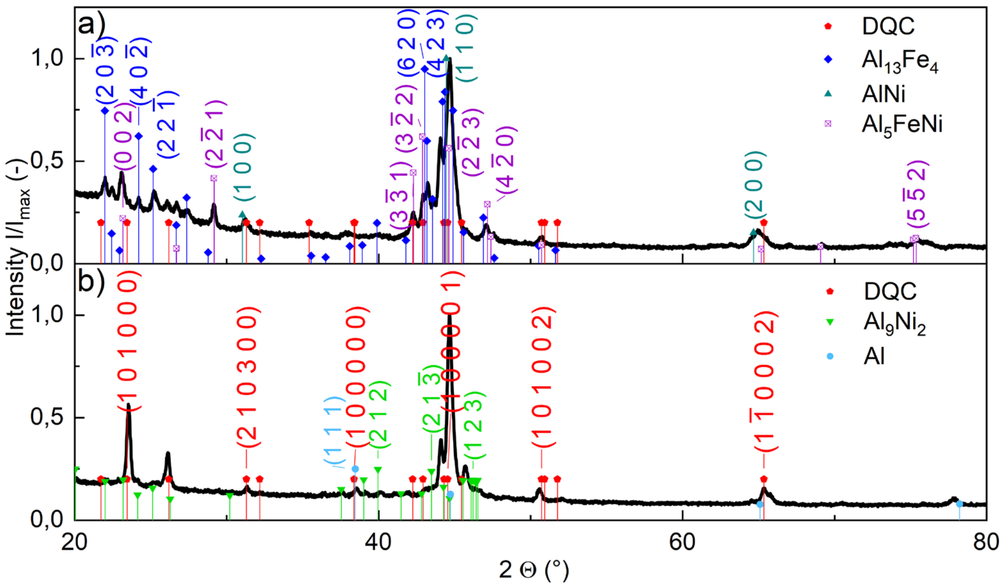

Fig. 2. X-ray diffractograms of $Al_{70}Ni_{15}Fe_{15}$ (ANF-1) (a) and $Al_{71.5}Ni_{23.5}Fe_5$ (ANF-2) (b) alloys in the pulverized form with marked positions of identified phases reflections

that the relative intensity of the reflections from DQC compared to those of the other phases is much higher than that of ANF-1, suggesting a dominant contribution of the quasicrystalline phase in the ANF-2 ribbon.

TEM images of the ANF-1 alloy in selected areas of the ribbon indicate the diverse morphology of this material. Fig. 3a shows eutectic (1) and neighbouring homogeneous grains of another phase (2). The selected area electron diffraction pattern obtained from the eutectic contains two systems of reflections that can be attributed to the $Al_{13}Fe_4$ and AlNi phases (Fig. 3b). The following crystallographic relationship between the phases can be described based on this diffraction: $[010]_{Al13Fe4}\|[110]_{AlNi}$ and $(20\text{-}6)_{Al13Fe4}\|(1\text{-}10)_{AlNi}$. The grain visible next to the eutectic was identified as the Al_5FeNi phase (Fig. 3c). Another fragment of the ribbon contained equiaxed grains (Fig. 3d), which were identified based on electron diffraction as $Al_{13}Fe_4$ and DQC phases (Fig. 3e, f). The phase composition of the ANF-1 alloy is similar to $Al_{72.5}Fe_{14.5}Ni_{13}$ as-cast alloy, which contained a decagonal quasicrystal and Al_5FeNi intermetallic phase [16]. On an equilibrium phase diagram at 800°C, all the identified crystalline phases occurred adjacent to the decagonal quasicrystal [17].

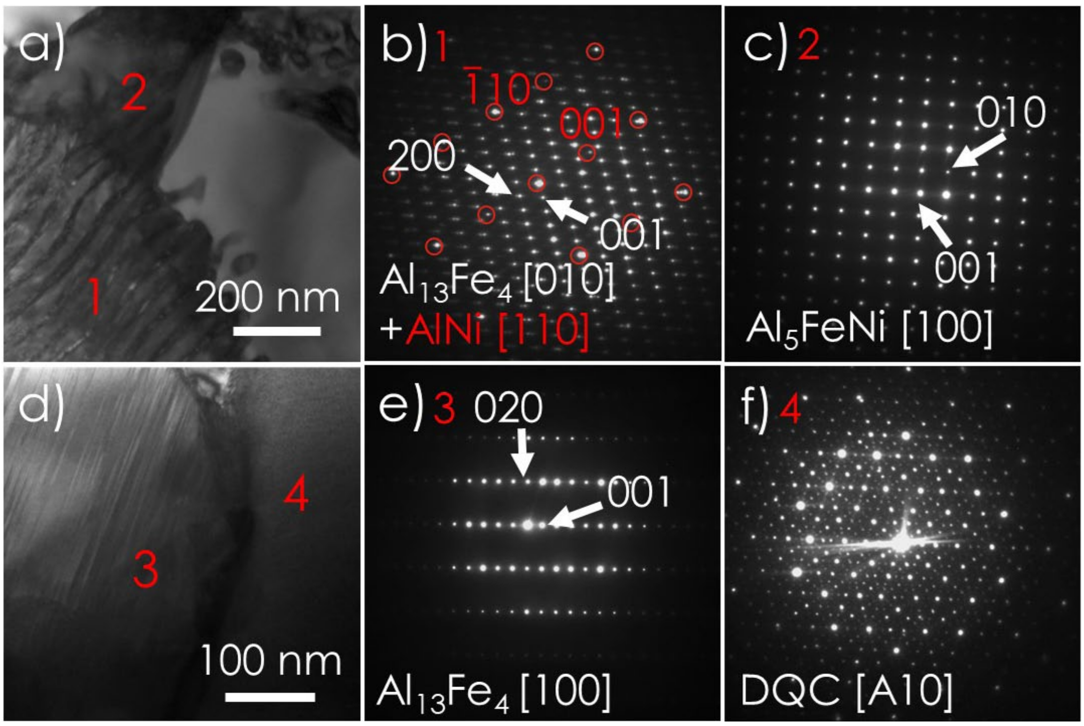

Fig. 3. Bright field TEM microstructure acquired for two fragments of $Al_{70}Ni_{15}Fe_{15}$ (ANF-1) melt-spun ribbon revealing morphological diversity occurring in the material (a, d) with electron diffractions from the indicated points: 1 – $Al_{13}Fe_4$ + AlNi (b); 2 – Al_5FeNi (c); 3 – $Al_{13}Fe_4$ (e); 4 – DQC (f)

The ANF-2 alloy also has a complex morphology (Fig. 4a, d). Areas with a homogeneous matrix containing globular precipitates with sizes of several hundred nanometres were observed (Fig. 4a). The selected area electron diffraction patterns acquired in the matrix region indicate the presence of a decagonal quasicrystal. Example diffraction patterns with characteristic tenfold [A10] and twofold symmetry [A2] are presented in Fig. 4b, c, while the spherical precipitates were identified as the Al_9Ni_2 phase (Fig. 4f). The EDS analysis showed that the quasicrystals composition is Al-73 at.%, Ni-20 at.%

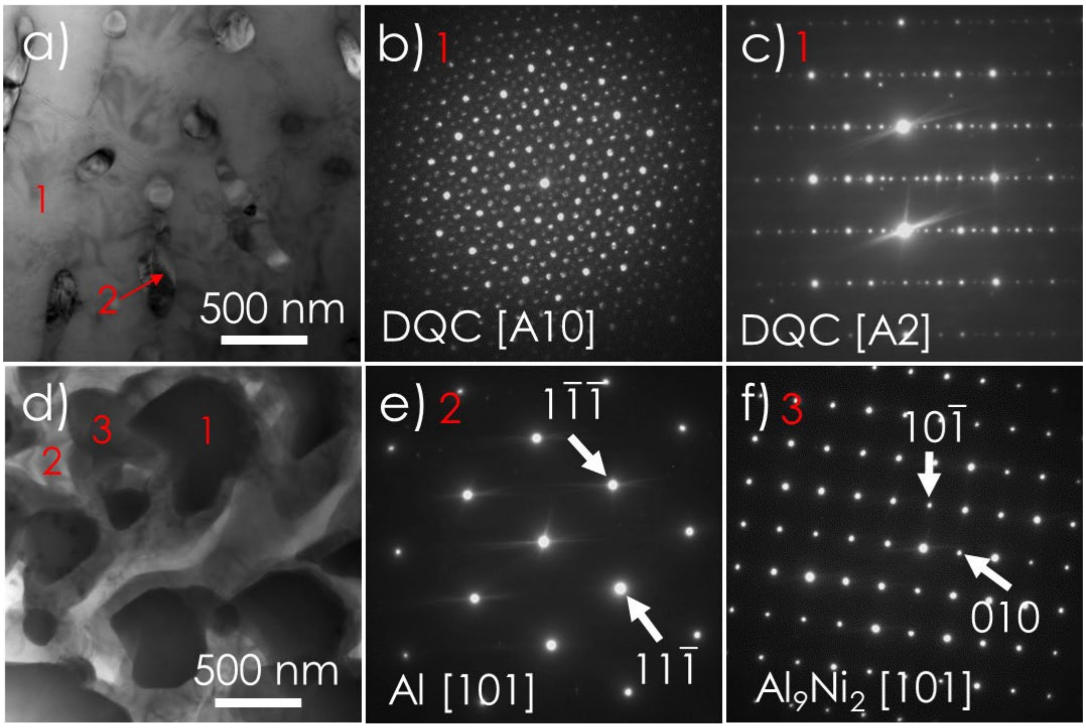

Fig. 4. Bright-field TEM images (a, d) of the $Al_{71.5}Ni_{23.5}Fe_5$ (ANF-2) melt-spun ribbon with electron diffractions of identified phases: DQC (b, c), and α-Al (e), Al_9Ni_2 (f)

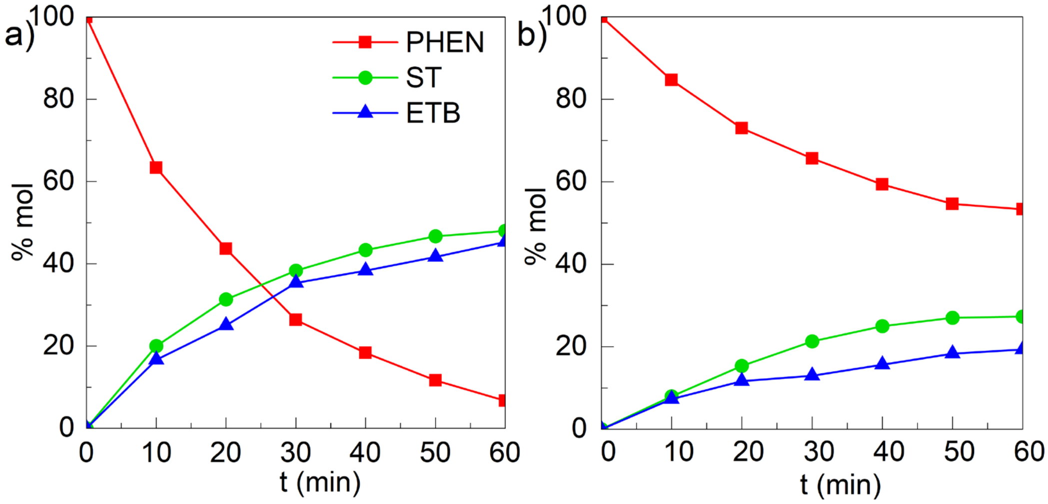

Fig. 5. Results of catalytic tests in phenylacetylene hydrogenation reactions for $Al_{70}Ni_{15}Fe_{15}$ (ANF-1) powder (a) and $Al_{71.5}Ni_{23.5}Fe_5$ (ANF-2) powder (b). PHEN – concentration of phenylacetylene, ST – concentration of styrene, ETB – concentration of ethylbenzene

and Fe-7 at.%. In other fragments of the ribbon, quasicrystal grains surrounded by the Al_9Ni_2 phase were observed (Fig. 4d), with an α-Al solid solution between them (Fig. 4e). The phase composition of the alloy varied from the rapidly solidified plates with the same chemical composition, which contained quasicrystal, Al_3Ni_2, and Fe(Al,Ni) phases [2]. The $Al_9(Ni,Fe)_2$ phase was obtained after the isothermal annealing at 800°C in the alloy $Al_{71}Ni_{24}Fe_5$ and occurs in equilibrium with decagonal quasicrystal and intermetallic phases. Below this temperature the decagonal quasicrystalline phase does not exist [17].

Despite the selection of two compositions in the expected range of decagonal quasicrystal [17], multiphase alloys were obtained for both studied ribbons. These results indicate the necessity of optimisation melt spinning process in terms of wheel linear speed, gas pressure and nozzle diameter. Increasing the linear speed of the wheel should lead to the formation of thinner ribbons and higher cooling rates, resulting in a more homogeneous material [20].

3.2. Evaluation of catalytic performance

The catalytic properties of investigated materials were evaluated in the phenylacetylene hydrogenation reaction. Directly before reactions the powdered ribbons were cleaned with $NaBH_4$ aqueous solution. Both materials revealed catalytic activity in the applied reaction conditions and the results of tests are presented in Fig. 5. For ANF-1 alloy, after 1 h the degree of phenylacetylene conversion exceeded 90%. This reaction also resulted in a conversion to styrene of approximately 45%, which ensured selectivity to this product of over 50% at the end of the reaction. ANF-2 alloy provided the substrate conversion of 46% and selectivity to styrene over 50%. However, considering the reaction mixture composition changes, after a longer reaction time it should be possible to achieve higher phenylacetylene conversion. Higher share of iron in ANF-1 alloy and presence of monoclinic $Al_{13}Fe_4$ phase may be factors providing better catalytic performance than in case of ANF-2 alloy [14]. However, to determine the impact of material composition on catalytic performance, the examination of single phase alloys is necessary. The catalytic performance of Al-Ni-Fe melt-spun alloys can be compared to results obtained under the same conditions for the Al-Ni-Co single-phase quasicrystalline alloy [12] and Al-Cu-Co multiphase alloy [21]. $Al_{70}Ni_{15}Co_{15}$ quasicrystal, produced in the form of melt-spun ribbons, achieved a conversion rate of approximately 80%, with selectivity to styrene of 50 This performance is comparable to that of the ANF-1 alloy, which contains the same concentration of transition metals [12]. Meanwhile, the ANF-2 alloy exhibited similar reaction results to the $Al_{65}Cu_{15}Co_{20}$ multiphase alloy, which included both decagonal quasicrystal and intermetallic phases. The Al-Cu-Co alloy provided a conversion rate for phenylacetylene of about 45%, with selectivity to styrene of 60% [21]. The high substrate conversion obtained for multiphase ANF-1 alloy suggest that the higher impact on catalytic performance have alloy composition than defined single-phase structure and alloys containing high concentration of cobalt and iron provide better catalytic performance than alloys with other transition metals.

4. Conclusions

Two Al-Ni-Fe alloys ($Al_{70}Ni_{15}Fe_{15}$ and $Al_{71.5}Ni_{23.5}Fe_5$) manufactured by the melt spinning method exhibit complex microstructures and multiphase composition that contained decagonal quasicrystal and intermetallic phases.

Both materials revealed catalytic activity in the reaction of phenylacetylene hydrogenation. Higher substrate conversion, exceeding 90%, and selectivity to styrene over 50% was obtained for the alloy with composition $Al_{70}Ni_{15}Fe_{15}$. ANF-2 alloy achieved a substrate conversion of 46% and over 50% selectivity to styrene. The higher catalytic properties may result from a higher concentration of iron in the alloy than in the other one, which provides high catalytic performance for Al-Fe intermetallic phases.

Acknowledgements

This work was financially supported by the National Science Centre Poland (NCN) within project No. 2021/41/N/ST8/02533.

REFERENCES

[1] J.M. Dubois, Properties and applications of quasicrystals and complex metallic alloys. Chem. Soc. Rev. **41**, 6760-6777 (2012). DOI: https://doi.org/10.1039/c2cs35110b

[2] R. Babilas, K. Młynarek, W. Łoński, M. Lis, D. Łukowiec, M. Kądziołka-Gaweł, T. Warski, A. Radoń, Analysis of thermodynamic parameters for designing quasicrystalline Al-Ni-Fe alloys with enhanced corrosion resistance. J. Alloys Compd. **868**, 159241 (2021). DOI: https://doi.org/10.1016/j.jallcom.2021.159241

[3] M. Krajčí, J. Hafner, Catalytic Properties of Five-Fold Surfaces of Quasicrystal Approximants. Aperiodic Crystals 269-274 (2013). DOI: https://doi.org/10.1007/978-94-007-6431-6_36

[4] Y. Yang, M. Wei, Intermetallic compound catalysts: Synthetic scheme, structure characterization and catalytic application. J. Mater. Chem. A **8**, 2207-2221 (2020). DOI: https://doi.org/10.1039/c9ta09448b

[5] M. Armbrüster, Intermetallic compounds in catalysis–a versatile class of materials meets interesting challenges. Sci. Technol. Adv. Mater. **21**, 303-322 (2020). DOI: https://doi.org/10.1080/14686996.2020.1758544

[6] L. Piccolo, C. Chatelier, M.C. De Weerd, F. Morfin, J. Ledieu, V. Fournée, P. Gille, E. Gaudry, Catalytic properties of Al13TM4 complex intermetallics: influence of the transition metal and the surface orientation on butadiene hydrogenation. Sci. Technol. Adv. Mater. **20**, 557-567 (2019). DOI: https://doi.org/10.1080/14686996.2019.1608792

[7] A. Zięba, K. Stan-Głowińska, Ł. Rogal, G. Cios, P. Czaja, J. Przewoźnik, R. Chulist, D. Duraczyńska, E.M. Serwicka, L. Lityńska-Dobrzyńska, Microstructure and catalytic properties of rapidly solidified Al-28.5 at% Fe and Al-28.5 at% Co alloys applied for selective hydrogenation of phenylacetylene. Mater. Today Commun. **33**, 104422 (2022). DOI: https://doi.org/10.1016/j.mtcomm.2022.104422

[8] T. Tanabe, S. Kameoka, A.P. Tsai, Microstructure of leached Al-Cu-Fe quasicrystal with high catalytic performance for steam reforming of methanol. Appl. Catal. **384**, 241-251 (2010). DOI: https://doi.org/10.1016/j.apcata.2010.06.045

[9] E. Gaudry, C. Chatelier, D. Loffreda, D. Kandaskalov, A. Coati, L. Piccolo, Catalytic activation of a non-noble intermetallic surface through nanostructuration under hydrogenation conditions revealed by atomistic thermodynamics. J. Mater. Chem. A **8**, 7422-7431 (2020). DOI: https://doi.org/10.1039/d0ta01146k

[10] K. Abe, R. Tsukuda, N. Fujita, S. Kameoka, High catalytic performance of Al-Pd-(Ru, Fe) icosahedral approximants for acetylene semi-hydrogenation. RSC Adv. **11**, 15296-15300 (2021). DOI: https://doi.org/10.1039/d1ra01958a

[11] M. Yoshimura, A.P. Tsai, Quasicrystal application on catalyst. J. Alloys Compd. **342**, 451-454 (2002). DOI: https://doi.org/10.1016/S0925-8388(02)00274-8

[12] A. Zięba, K. Stan-Głowińska, D. Duraczyńska, M. Marzec, A. Góral, P. Czaja, Ł. Rogal, L. Lityńska-Dobrzyńska, Al-Ni-Co decagonal quasicrystal application as an energy-effective catalyst for phenylacetylene hydrogenation. Sustainable Mater. Technol. **41**, e01055 (2024). DOI: https://doi.org/10.1016/j.susmat.2024.e01055

[13] J.N. Barbier, N. Tamura, J.L. Verger-Gaugry, Monoclinic Al13Fe4 approximant phase: a link between icosahedral and decagonal phases. J. Non Cryst. Solids **153-154**, 126-131 (1993). DOI: https://doi.org/10.1016/0022-3093(93)90328-U

[14] M. Armbrüster, K. Kovnir, M. Friedrich, D. Teschner, G. Wowsnick, M. Hahne, P. Gille, L. Szentmiklósi, M. Feuerbacher, M. Heggen, F. Girgsdies, D. Rosenthal, R. Schlögl, Y. Grin, Al13Fe4 as a low-cost alternative for palladium in heterogeneous hydrogenation. Nat. Mater. **11**, 690-693 (2012). DOI: https://doi.org/10.1038/nmat3347

[15] B. Grushko, T.Ya. Velikanova, Stable and metastable quasicrystals in Al-based alloy systems with transition metals. J. Alloys Compd. **367**, 58-63 (2004). DOI: https://doi.org/10.1016/j.jallcom.2003.08.012

[16] J.B. Qiang, D.H. Wang, C.M. Bao, Y.M. Wang, W.P. Xu, M.L. Song, C. Dong, Formation rule for Al-based ternary quasicrystals: Example of Al-Ni-Fe decagonal phase. J. Mater. Res. **16**, 2653-2660 (2001). DOI: https://doi.org/10.1557/jmr.2001.0364

[17] B. Grushko, U. Lemmerz, K. Fischer, C. Freiburg, The low-temperature instability of the decagonal phase in Al-Ni-Fe. Phys. Status Solidi A **155**, 17-30 (1996). DOI: https://doi.org/10.1002/pssa.2211550103

[18] X. Zhang, A. Atrens, Rapid solidification characteristics in melt spinning. Mater. Sci. Eng. A **159**, 243-251 (1992). DOI: https://doi.org/10.1016/0921-5093(92)90295-C

[19] J. Grin, U. Burkhardt, M. Ellner, K. Peters, Refinement of the Fe4Al13 structure and its relationship to the quasihomological homeotypical structures. Z. Kristallogr. - New Cryst. Struct. **209**, 479-487 (1994). DOI: https://doi.org/10.1524/zkri.1994.209.6.479

[20] V.I. Tkatch, A.I. Limanovskii, S.N. Denisenko, S.G. Rassolov, The effect of the melt-spinning processing parameters on the rate of cooling. Mater. Sci. Eng. A **323**, 91-96 (2002). DOI: https://doi.org/10.1016/S0921-5093(01)01346-6

[21] A. Zięba, K. Stan-Głowińska, D. Duraczyńska, L. Lityńska-Dobrzyńska, Rapidly solidified Al-Cu-Co quasicrystalline alloy: microstructure and catalytic properties. Arch. Civ. Mech. Eng. **24**, 127 (2024). DOI: https://doi.org/10.1007/s43452-024-00904-x